Med. & Biol. Eng. & Comput., 1983, 21, 343–350

Optimal QRS detector

N.V. Thakor* **J. G. Webster** **W. J. Tompkins**

Department of Electrical and Computer Engineering, University of Wisconsin-Madison, Madison, WI 53706

Abstract—*The problem of detecting the QRS complex in the presence of noise was analysed. Most QRS detectors contain a filter to improve the signal-to-noise ratio and compare the signal with a threshold. In an earlier paper we identified an optimal filter. Various techniques to generate threshold and detector designs were studied. Automatic gain-control circuits with a fixed threshold have a very slow response to different rhythms. Automatic threshold circuits based on simple peak-detection schemes have a fast response, but are very sensitive to sudden variations in QRS amplitudes and noise transients. None of the methods described to date present any optimisation criteria for detecting the signal (QRS complex) in the presence of noise. The probabilities of FPs (false positives) and FNs (false negatives) were investigated and an optimised threshold criterion based on FP/FN was developed. Presently, data are being collected to compare various techniques from their ROC (receiver operating characteristics).*

Keywords—*Circuits, Complex, Detectors, Electrocardiography, Electronics, QRS, ROC techniques*

1 Introduction

WE INTERPRET the e.c.g. by identifying near-periodic events with characteristic morphologies. The QRS complex is the most prominent feature of the e.c.g. Hence e.c.g. interpretation techniques rely primarily on QRS detectors. But QRS detection is complicated by two factors: (i) There is a wide variation in QRS morphologies and rhythms, especially in abnormal e.c.g.s (ii) Noise from various sources may corrupt the e.c.g. recording. For a given individual, QRS rhythm shows variations due to respiration, exercise and other factors. When comparing normal individuals, QRS morphologies show slight but distinct variations. On the other hand, we can distinguish abnormal e.c.g.s because of their quite different rhythms and/or morphologies. For example, a paced QRS beat has a longer duration than a normal sinus beat. A burst of rapidly occurring beats identifies tachycardia. A p.v.c. (premature ventricular contraction) shows both rhythm and morphological variation. It occurs early in a normal QRS cycle and may also be wide and inverted. A QRS detector must adapt to rapid or sudden rhythm changes. It must also detect normal as well as abnormal beats. In addition, the e.c.g. may be corrupted with noise. 60 Hz power lines add interference to e.c.g. recordings. Movement of electrodes with respect to skin causes motion artefact. Respiration and slow movement such as bending causes baseline drift. E.m.g. (muscle noise) adds high-frequency noise. This noise results in false or extra QRS detection which results in a FP (false positive). On the other hand a FN (false negative) occurs when the QRS detector fails to detect a normal or an abnormal beat. We evaluate the performance of QRS detectors by counting FPs and FNs.

BRYDON (1976) reviews the research on QRS detection. Typically a QRS detector consists of a filter stage followed by a linear or nonlinear detection stage. The QRS filter should maximise the signal (QRS) to noise (e.m.g., motion artefact, T wave) ratio. THAKOR *et al.* (1980) present the theory of an optimal QRS filter and recommend a bandpass filter with a 17 Hz centre frequency and a Q of 4. There are a variety of QRS detection techniques. FRADEN and NEUMAN (1980) use automatic-gain-control (a.g.c.) followed by a comparator with hysteresis. The Hewlett-Packard Co. (see References) uses a fast-reacting, peak-detecting, and decaying threshold circuit. GEBBEN and WEBB (1973) use automatic sensitivity control to adjust the detection threshold. Others use linear and nonlinear techniques such as differentiation, squaring and pulse-width discrimination (BRYDON, 1976), low-level clipping (FRADEN and NEUMAN, 1980), and contour limiting (GOOVAERTS *et al.*, 1976). These result in a more complex design, although there is no evidence that they lead to significant improvement in performance.

* *Now with the Department of Electrical Engineering and Computer Science, Northwestern University, Evanston, IL 60201, USA*

First received 7th July, 1982

0140–0118/83/030343+08$01·50/0

This paper analyses the design of an optimal detector. We assume that a linear or nonlinear signal-processing technique has filtered and processed the e.c.g. The next stage is a detector unit consisting of (i) a level-identification circuit, such as a peak detector, (ii) a threshold-setting circuit, and (iii) a comparator. The output of the comparator signals the QRS pulse. The following detection techniques are reviewed: (*a*) fixed threshold, (*b*) a.g.c., and (*c*) automatic threshold (a.t.). We describe a signal-detection technique that optimises the QRS detection based on the FP/FN (false positive/false negative) criteria. An analogue circuit implementation and computer simulation result is described. We compare and evaluate various techniques by their ROC (receiver operating characteristics) data.

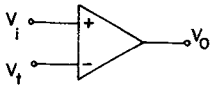

Fig. 1 *Fixed threshold (value V_t) detector*

2 Detection techniques

2.1 *Fixed threshold*

Fig. 1 shows a simple detector. It is based on a comparator that compares the e.c.g. signal (V_i) with a preset threshold voltage (V_t) (LAW *et al.*, 1979). The rule for detecting the event (V_o) is

$$V_o = 1 \text{ if } V_i > V_t$$
$$= 0 \text{ if } V_i \leqslant V_t \quad . \quad . \quad . \quad . \quad . \quad . \quad . \quad . \quad (1)$$

This scheme has limitations: (i) It does not take into account variations in the signal amplitudes (ii) A preset threshold is difficult to optimise. Too low a threshold makes the detector sensitive to noise, although it may detect the signal well. Conversely, too high a threshold improves noise immunity at the cost of missing some events.

Typically these limitations are resolved by one of two techniques: (*a*) variable gain control or (*b*) variable threshold. Variable gain control may be manual (crude) or automatic. An automatic gain control (a.g.c.) circuit relies on some previous knowledge of the signal amplitude. An average value obtained from the previous few cycles is used to control the gain of the amplifier stage (FRADEN *et al.*, 1980). Variable threshold on the other hand may detect the peak signal value from the previous cycle and utilise a certain fraction of that level to detect the subsequent QRS complex (HEWLETT PACKARD, 1975).

2.2 *Automatic gain-control (a.g.c.) circuit*

Fig. 2 shows a circuit that detects the QRS using a.g.c. The input V_i to the a.g.c. circuit is the filtered and rectified e.c.g. The peak detector output V_o' is proportional to the output voltage V_o and controls the channel resistance R_d of the j.f.e.t. The drain-to-source

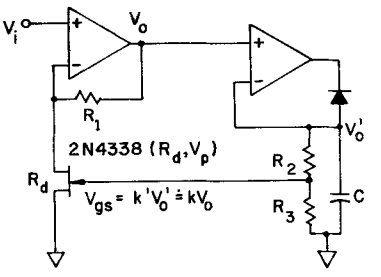

Fig. 2 *A.g.c. circuit*

resistance of a j.f.e.t. is proportional to the gate-to-source voltage V_{gs}. For our circuit

$$R_d = R_0 V_p/(V_p - V_{gs}) \quad . \quad . \quad . \quad . \quad . \quad . \quad . \quad (2)$$

where R_0 is the channel resistance when $V_{gs} = 0$, and V_p is the pinch-off voltage. The gain of the amplifier is

$$A_v = 1 + (R_1/R_0 V_p)(V_p - V_{gs}) \quad . \quad . \quad . \quad . \quad . \quad (3)$$

Hence the output of the a.g.c. circuit is

$$V_o = [1 + (R_1/R_0)]\, V_i/[1 + (kR_1/R_0 V_p) V_i]$$
$$= \text{constant, if } R_1 \gg R_0 \quad . \quad . \quad . \quad . \quad . \quad . \quad (4)$$

Fig. 3 shows the waveforms of the original signal, and the a.g.c. circuit output. The a.g.c. circuit has a wide dynamic range and works well for fast repetitive events such as sinusoidally varying radio signal. But the e.c.g. is characterised by a sharp pulse followed by about a 1 s pause. Thus, the circuit requires a time constant of at least 10 s for the peak detector to maintain a fairly

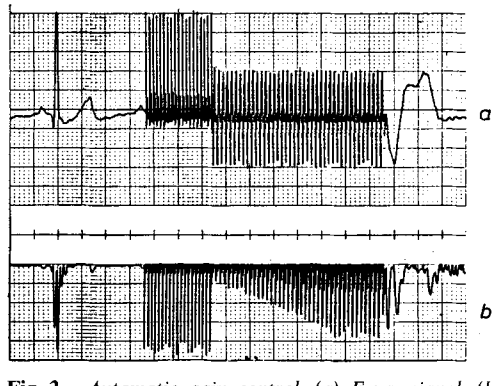

Fig. 3 *Automatic gain control. (a) E.c.g. signal. (b) The filtered and rectified e.c.g. signal at the output of the a.g.c. circuit. The waveforms show normal e.c.g. followed by paced rhythm. (Chart speed 25 divisions per second or 1 division per second)*

uniform value of the control voltage V_{gs} between two QRSs.

The a.g.c. circuit does not respond fast enough to accommodate the sudden changes in amplitude that occur with p.v.c.s or paced rhythm with intermittent capture. Also unwanted low-amplitude signals such as T waves are disproportionately amplified, which may result in false detections.

2.3 *Automatic threshold circuit*

The circuit in Fig. 4 shows an alternate approach. A change in signal amplitude does not vary the amplifier gain, but instead varies the threshold. This scheme shortens the adaptation time. The amplitude of the

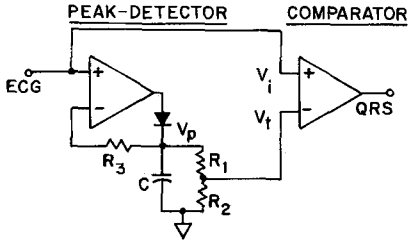

Fig. 4 *Automatic threshold circuit*

preceding QRS complex determines the new threshold. The first operational amplifier acts as a half-wave rectifier and a peak detector. As the charging time constant is very small, capacitor C quickly assumes a voltage corresponding with the previous signal peak. During the discharge cycle, the time constant $\tau = (R_1 + R_2)C = 5$ s. The threshold V_t is a fraction of the previous peak value V_p.

$$V_t = [R_2/(R_1 + R_2)]\, V_p \exp(-t/\tau) \quad . \quad . \quad . \quad (5)$$

Although this circuit responds faster than an a.g.c. circuit, it is highly sensitive to beat-by-beat variations and transients. For example, a transient or even a high

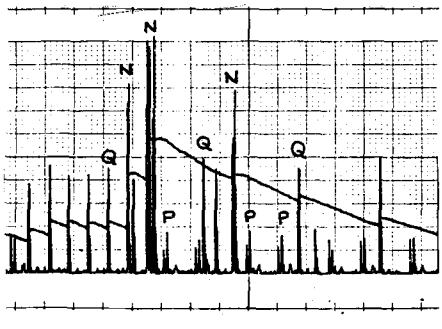

Fig. 5 *Filtered and rectified e.c.g. input V_i and the exponentially decaying threshold V_t from the automatic threshold circuit. Chart speed 5 divisions per second (Q—normal QRS, P—paced QRS, and N—noise)*

previous beat can drive the threshold quite high, since it depends only on the previous peak value (Fig. 5). A smaller discharge time constant could reduce the threshold quickly, but it would get too low and triggering could occur on small artefacts and P waves.

An improved circuit uses a sample-and-hold detector that retains the fast response of the automatic threshold circuit, while overcoming some of its limitations (THAKOR and WEBSTER, 1981). Instead of charging the threshold to the full peak of the previous beat, it charges only during a 10 ms period at the beginning of a QRS complex. Because the sampling period is small, the sudden transients cannot cause the threshold to go too low. A hold circuit holds the threshold until the next QRS. This circuit works well for variations in QRS amplitude. However, in the presence of high noise, false detections occur.

An optimised detection technique should take into account the signal amplitude distribution as well as the noise distribution. A high threshold results in greater noise immunity but more missed QRSs. Therefore there will be more FNs. On the other hand a low threshold detects all QRSs and also more artefacts. Therefore there will be more FPs. An optimal detector then depends on a selected FP/FN ratio and the statistical distribution of the e.c.g. signal as well as the noise (THAKOR, 1981). We now describe the theory behind an optimised detector and an evaluation.

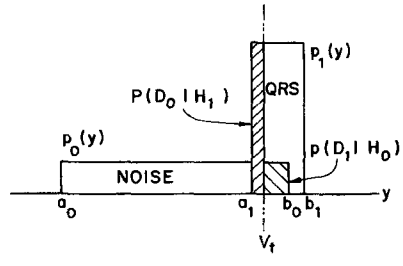

Fig. 6 *Noise and QRS amplitude distributions and optimal threshold*

2.4 *Optimised statistical detection*

Fig. 6 shows our model of QRS and noise amplitude distributions. Signals are filtered and rectified and therefore lie in the range from $a_0 = 0$ V to the +5 V supply voltage. We can readily detect the peak value of noise and therefore obtain a very good estimate of b_0. Similarly another peak-detector determines b_1, peak value of the QRS. Fig. 6 is the plot of amplitude distributions of the peak value of the QRS and the highest noise amplitude for a complete e.c.g. cycle. Respiratory modulation causes about 15% variation in the QRS amplitude. Differences between normal and abnormal QRS morphologies may cause amplitude variations as large as 70% as in Fig. 5, but this is rare. Therefore we estimate a total variation of 20%, and $a_1 = 0{\cdot}8b_1$. These assumptions provide us a model for amplitude distributions from which we calculate the QRS detection threshold V_t. Our

objective is to minimise FPs and FNs. Many criteria exist for such an optimisation. For a hypothesis H_0 that noise is present and H_1 that a QRS is present, we make either the decision D_0 that noise is present or D_1 that a QRS is present. Then $P(D_0 \mid H_1)$ is the probability of FN and $P(D_1 \mid H_0)$ is the probability of FP. We define C_{ij} as the cost associated with choosing the hypothesis H_i when actually the hypothesis H_j is true. Baye's criterion (WHALEN, 1971) calculates the average cost associated with the decision to select H_0 or H_1.

$$C' = P(H_0)[P(D_0 \mid H_0)C_{00} + P(D_1 \mid H_0)C_{10}] + [1 - P(H_0)][P(D_0 \mid H_1)C_{01} + P(D_1 \mid H_1)C_{11}] \quad . \quad . \quad . \quad . \quad (6)$$

But minimisation of Baye's cost requires prior knowledge of $P(H_0)$. The minimax criterion (WHALEN, 1971) does not require such prior information. The minimax criterion minimises the worst-case cost of a wrong decision. This may not result in the least cost, but in the absence of prior knowledge of $P(H_0)$ it limits the risk of a wrong decision. Differentiating C' with respect to $P(H_0)$ yields

$$C_{10}P(D_1 \mid H_0) + C_{00}P(D_0 \mid H_0) = C_{01}P(D_0 \mid H_1) + C_{11}P(D_1 \mid H_1) \quad . \quad (7)$$

We assume that the costs C_{00} and C_{11} are zero. Therefore

$$P(D_1 \mid H_0)/P(D_0 \mid H_1) = C_{01}/C_{10} = k \quad . \quad . \quad (8)$$

Now $P(D_1 \mid H_0)$ is the ratio of the number of e.c.g. cycle with noise pulses exceeding the threshold (false positives) to total number of e.c.g. cycles, and $P(D_0 \mid H_1)$ is the ratio of the number of e.c.g. cycles with QRS complexes below the threshold (false negatives) to the total number of e.c.g. cycles. Therefore

$$\frac{P(D_1 \mid H_0)}{P(D_0 \mid H_0)} = \frac{\text{Number of false positives}}{\text{Number of false negatives}} = \frac{\text{FP}}{\text{FN}} = k$$

We minimise the cost of false detection by selecting a proper FP/FN ratio.

$$\int_{V_t}^{b_0} p_0(y)dy = k \int_{a_1}^{V_t} p_1(y)dy \quad . \quad . \quad . \quad . \quad . \quad (9)$$

For example, if we choose $k = 1$, we equate the shaded areas. For other possible values of k

$$\begin{aligned} (V_t - a_1)/(b_1 - a_1) &= k(b_0 - V_t)/(b_0 - a_0) \\ V_t &= [a_1(b_0 - a_0) + kb_0(b_1 - a_1)]/[(b_0 - a_0) + k(b_1 - a_1)] \\ &= [1 + (k-1)c](b_0 b_1)/(b_0 + kcb_1) \\ &\quad \text{for } a_0 = 0 \text{ and } c = (b_1 - a_1)/b_1 \end{aligned} \quad (10)$$

Fig. 7 shows the computer simulation of this equation. We plot the threshold for five different levels of QRS amplitude and three cases of FP/FN. For each case of QRS amplitude and FP/FN we calculate the threshold level, as the noise from 0 V to the maximum value of 5 V was increased. Fig. 7 shows the noise with increasing dashed lines and the threshold with curved solid lines. For example in column four, the QRS amplitude is uniformly distributed from a_1 to b_1 volts, with a mean value of 4 V. The noise level from 0 V to 5 V (increasing dashed line) was increased. Three curves for threshold (solid curved lines) were plotted for three different value of FP/FN. Fig. 6 shows that for case $a_1 < b_0 < b_1$, then V_t is slightly greater than the lower limit of the QRS, a_1. Fig. 7 duplicates this case: when the noise maximum b_0 (increasing dashed line) is greater than the lower limit of the QRS (horizontal solid line), then the threshold (curved solid lines) is somewhere in between. The threshold depends on the FP/FN criterion. As long as the noise amplitude is smaller than the lower limit (a_1) of the QRS amplitude, the threshold for FP/FN = 2 is somewhat lower than for FP/FN = 0·5. This is because a lower threshold (FP/FN = 2) permits more FPs while a higher threshold (FP/FN = 0·5) permits more FNs. We implement eqn. 10 with a multiplier/divider circuit using j.f.e.t.s as voltage-controlled resistors.

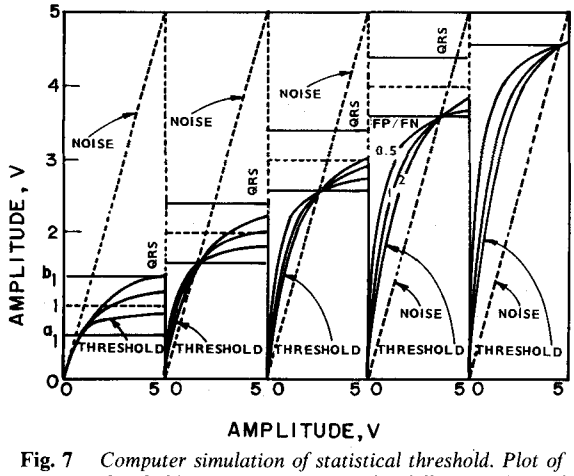

Fig. 7 *Computer simulation of statistical threshold. Plot of threshold (curved solid lines) for different values of noise voltage (increasing dashed lines). Plots repeated for five values of QRS amplitude and three cases of FP/FN*

3 QRS detector circuit

Fig. 8 shows the circuit diagram of the statistically optimised QRS detector. F.e.c.g. is the output of a

bandpass filter and full-wave rectifier. Operational amplifier A is the QRS peak (b_1) detector and B is the noise peak (b_0) detector. We implement eqn. 10 with operational amplifiers C, D and E and a matched-pair

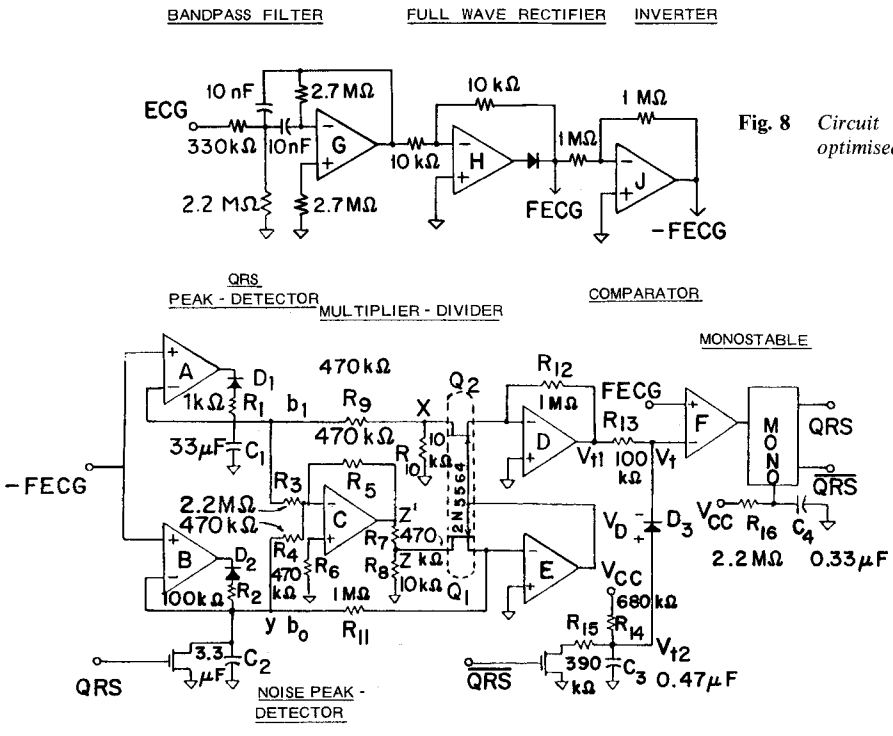

Fig. 8 *Circuit diagram of statistically optimised QRS detector*

and an exponentially decaying component that maintains a high threshold when V_{t1} is reset during the QRS pulse ($V_{t1} = 0$ because $b_0 = 0$ when QRS = 1). The comparator F compares f.e.c.g. with V_t and

j.f.e.t. 2N5564. GRAEME (1973) shows that this circuit implements a function $-XY/Z$ by using the f.e.t.s as voltage-controlled resistors. Input voltage Z sets the drain-to-source voltage of Q_1. Input voltage Y sets the current Y/R_{11} which flows through Q_1. Operational amplifier E forces the gate voltage to set the required drain-to-source resistance $R_{11}Z/Y$. Operational amplifier E also drives the matched f.e.t. Q_2 to the same drain-to-source resistance. Therefore the current through Q_2 is $-X/(R_{11}Z/Y)$ and the output voltage of the operational amplifier D is $R_{12}XY/(R_{11}Z)$. Signals b_1 and Z' are attenuated so that the voltage drops across the f.e.t.s are less than 100 mV for linear operation. For $R_7 = R_9$ and $R_8 = R_{10}$

$$V_{t1} = \frac{R_{12}}{R_{11}} \frac{b_1 b_0}{(R_5/R_3)b_1 + (R_5/R_4)b_0} \quad . \qquad (11)$$

We show that $k = 1{\cdot}25$ leads to an optimal performance of the QRS detector. The respiratory modulation causes about 20% variation in the QRS amplitude. Therefore we implement eqn. 10 for $k = 1{\cdot}25$ and $c = 0{\cdot}2$ by appropriate selection of R_3, R_4, R_5, R_{11} and R_{12} (Fig. 8). The actual threshold V_t is V_{t1} if $V_{t1} > V_{t2} - V_D$ and $V_{t2} - V_D$ if $V_{t1} \leqslant V_{t2} - V_D$. V_{t2} provides a minimum threshold $R_{15}V_{cc}/(R_{14}+R_{15})$ triggers the QRS monostable when f.e.c.g. $> V_t$. Figs. 9*a*–*c* show the waveforms of the filtered and rectified e.c.g. and the threshold for three values of FP/FN.

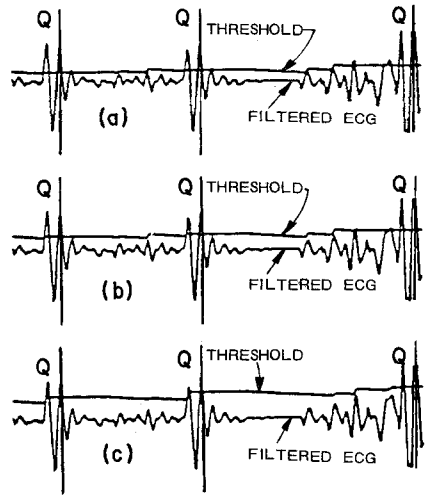

Fig. 9 *Filtered e.c.g. waveforms and three cases of the statistical threshold (V_{t1}). (a) FP/FN = 2 (b) FP/FN = 1, and (c) FP/FN = 0·5 (Q—filtered e.c.g.)*

4 Evaluation

All detector designs represent some form of compromise. High thresholds result in fewer FPs but more FNs. Low thresholds result in more FPs and fewer FNs. Selection of an optimal criterion depends on the application. For example, for exercise testing where high noise levels are expected, the threshold may be kept high. For bedside monitoring, the threshold may be kept low so that all significant events are captured. Hence the optimal design criterion can be chosen only after evaluating FP and FN rates for noisy data. Different design specifications of percentage TPs against percentage FPs provide such information. We plot TPs and FPs for various detection criteria (HANCOCK and WINTZ, 1966). For example, in Fig. 10*a* the detection curve traces a trajectory from the upper right corner to the lower left corner as the threshold level is raised. A number of detection curves were obtained by adding an increasing level of noise to the e.c.g. For the data in Figs. 10*a–d* we collected 12 segments of e.c.g. data (including various arrhythmias) from the Hewlett Packard tapes 14077 A-C, and altogether analysed 881 QRS complexes. We obtained five detection curves for each of the Figs. 10*a–d*, by adding five levels of band-limited (0·5–40 Hz) random noise to the e.c.g. We filtered the noisy e.c.g. with a bandpass filter with a centre frequency of 17 Hz and a Q of 3·3. We full-wave rectified the filtered e.c.g. and sampled it at 250 samples per second. We generated all the thresholds by computer simulation and automated the complete detection process. Thus five sets of noisy e.c.g. data were obtained, each consisting of 12 segments of arrhythmias with all sets having identical QRS annotations. For each detection curve we plot nine points for nine threshold values. For the fixed threshold (Fig. 10*a*) they represent nine threshold values, 0·2, 0·4, ..., 1·8 mV (referred to the input of the e.c.g. amplifier). We simulate the a.g.c. circuit and a fixed threshold by an adaptive threshold and fixed value of e.c.g. The threshold decays with a time constant of 20 s, which simulates slow adaptation. We obtain TP and FP rates for nine threshold levels of 10, 20, ..., 90% of the QRS peak. Fig. 10*c* shows the detection curves for the automatic threshold for a threshold decay time constant of 5 s and 10% to 90% of the QRS peak. Fig. 10*d* shows the detection curves for FN/FP = 0·2, 0·4, 0·6, 0·8, 1 and FP/FN = 0·2, 0·4, 0·6 and 0·8.

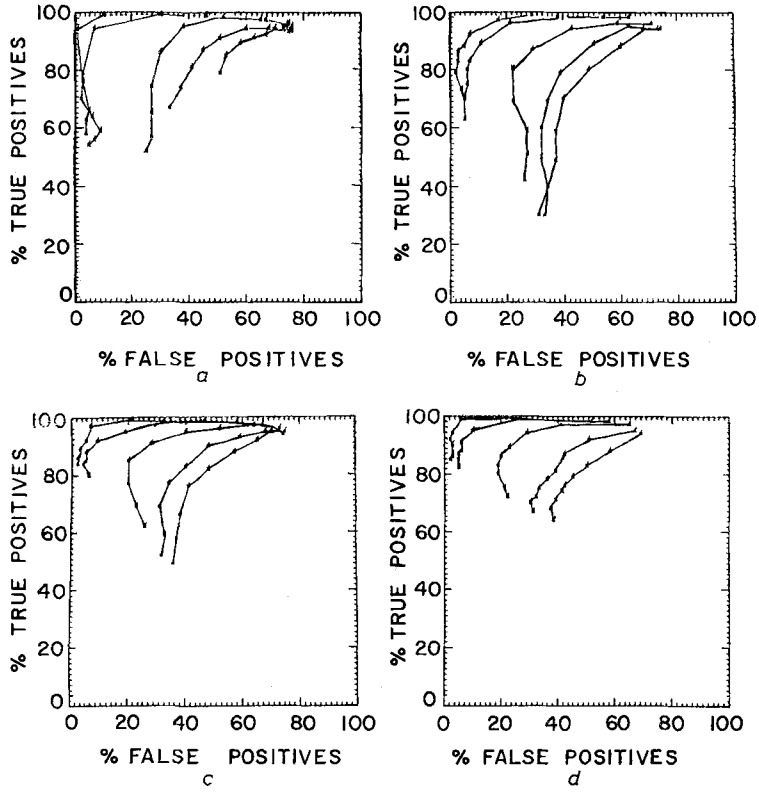

Fig. 10 *Detection curves for*
(a) the fixed threshold,
(b) the a.g.c.
(c) the automatic and
(d) the statistical threshold

The detection curves provide a very clear picture of the performance of various detector designs (HANCOCK and WINTZ, 1966). It was observed that the points at the upper left corner indicate the best performance. In fact the 'knee' of each curve represents the best compromise between TP rate and FP rate. Lower values of threshold result in high FP rates without significant improvement in TP rates. Higher

values of threshold result in a drop in TP rates without significantly dropping the FP rate. On that basis the following design criteria were selected.

Threshold = 0·8 mV for the fixed threshold detector

= 60% of QRS peak amplitude for the a.g.c. (τ = 20 s) and the automatic threshold detector (τ = 5 s)

FP/FN = 1·25 for the statistical threshold detector.

From Figs. 10*a–d* we conclude that the automatic threshold detector and the statistical threshold detector perform better than the others. The statistical threshold performs slightly better, especially under high noise conditions, as it can adapt to higher noise levels. It was observed that it performs even better in practice (although not indicated by our present data) when low-frequency noise is present from respiratory and motion artefacts. Since these are slower waveforms, the threshold has more time to adapt. This results in lower error rates on actual data, as compared to the simulated noise data. Most important, we can design the detector based on theoretically selected FP/FN performance criterion.

We evaluate the optimised QRS detector with an independent database consisting of about 10,000 QRS complexes. We recorded 7089 beats from 11 subjects during standard exercise protocol consisting of bending, weight lifting and jogging. We obtained 2986 beats from 100 Holter tapes of patients with variety of cardiac abnormalities. Thus our database consists of high levels and variety of artefact and noise. Also there are large number of abnormal looking QRS complexes. We found that the percentage false detection was less than 0·5%. We note that our database contained artefacts and abnormal QRS morphologies far in excess of that occurring in normal Holter recording. Hence the percentage false detection should be far lower in practice. The performance of this QRS detector was compared with three commercial units (Table 1). Although our design uses far fewer components, as it is intended to be a portable device (THAKOR, 1981) it nevertheless outperforms the commercial units.

QRS detector design has been a subject of considerable research. Each designer has adopted an arbitrary set of criteria for his design. Although many designs are quite innovative, there is no convincing rationale for adopting a particular technique. The design process is optimised. Various filtering and detection techniques are reviewed and a new theory for optimal filtering and detection is proposed. The design based on a large number of QRS complexes is optimised. We finally evaluate the QRS detector with an independent database. For a database consisting of a high level of artefacts and abnormal e.c.g.s, only 0·65% false detections occur. The optimised QRS detector outperforms commercial designs.

Acknowledgment—This work was supported in part by the National Institutes of Health under grant HL-25691 and in part by Public Health Service Research Career Development Award HL00765 from National Institute of General Medical Sciences to Willis J. Tompkins.

References

BRYDON, J. (1976) Automatic monitoring of cardiac arrhythmias. In *IEE Medical Electronics Monographs* 18–22, HILL, D. W. and WATSON, B. W. (Eds.), Peter Peregrinus, 27–41.

FRADEN, J. and NEUMAN, M. R. (1980) QRS wave detection. *Med. & Biol. Eng. & Comput.*, **18**, 125–132.

GEBBEN, V. D. and WEBB, Jr., J. A. (1973) Cardiac R-wave detector with automatic sensitivity control. NASA Technical Note TN D-7152.

Table 1. *Comparison of QRS detectors*

Type	Beats	BD	TEK	HP	AM
Exercise	7089				
FP		40	30	736	16
FN		0	0	0	19
Holter	2986				
FP		22	104	14	13
FN		57	117	517	19
QRS Total	10075				
FP+FN		119	251	1267	67
%		1·18	2·50	12·6	0·65

(BD: Becton Dickinson Model 219 TEK: Tektronix Model 414
HP: Hewlett Packard Model 78213 AM: Arrhythmia Monitor)

GOOVAERTS, H. G., ROSS, H. H., VAN DEN AKKER, T. J. and SCHNEIDER, G. (1976) A digital QRS detector based on the principle of contour limiting. *IEEE Trans. Biomed. Eng.*, **23**, 154–160.

GRAEME, J. G. (1973) *Applications of operational amplifiers.* McGraw-Hill, New York.

HANCOCK, J. C. and WINTZ, P. A. (1966) *Signal detection theory.* McGraw Hill, New York.

HEWLETT PACKARD CO. (1975) *ECG Cardiotach Module 78209A.* Instruction manual, Waltham, MA.

LAW, H. F., EPSTEIN, R. F. and EPSTEIN, M. A. (1979) High-resolution determination of the R-R interval. *Am. J. Physiol.*, **236**, 894–898.

THAKOR, N. V. (1981) Design, implementation, and evaluation of a microcomputer-based portable arrhythmia monitor. Ph.D. Thesis, Dept. Elect. Comput. Eng., Univ. Wisconsin, Madison, WI.

THAKOR, N. V. and WEBSTER, J. G. (1981) Design and evaluation of QRS and noise detectors for ambulatory ECG monitors. *Med. & Biol. Eng. & Comput.*, **20**, 709–714.

THAKOR, N. V., WEBSTER, J. G. and TOMPKINS, W. J. (1980) Optimal QRS filter. *IEEE Front. Eng. Health Care*, pp. 190–195.

WHALEN, A. D. (1971) *Detection of signals in noise.* Academic Press, London.